JOURNAL OF SOLID STATE CHEMISTRY 59, 159–167 (1985)

The Crystal Structure of $Mo_{0.975}Ti_{0.025}O_2$ between 24 and 900°C

M. GHEDIRA,* C. DO-DINH,† AND M. MAREZIO

Laboratoire de Cristallographie du CNRS, associé à l'Université Scientifique et Médicale de Grenoble 166 X, 38042 Grenoble Cédex, France

AND J. MERCIER

Laboratoire d'Etudes des Propriétés Electroniques des Solides du CNRS, associé à l'Université Scientifique et Médicale de Grenoble 166 X, 38042 Grenoble Cédex, France

Received September 24, 1984; in revised form January 9, 1985

The structure of $Mo_{0.975}Ti_{0.025}O_2$ has been refined from single-crystal X-ray data at room temperature, 300, 500, 700, and 900°C. The variation of the lattice parameters as a function of temperature has been measured up to 1100°C. The existence of the Mo–Mo bonds of second order across the shared octahedral edge is confirmed. The bond strength–bond length method of Zachariasen gives the correct valence for the cations, but yields 2.168 for O(1) and 1.832 for O(2). These unreal charges are attributed to the presence of the Mo–Mo double bonds. The same calculation applied to the isostructural VO_2 gives the correct valences for all atoms. The structure of $Mo_{0.975}Ti_{0.025}O_2$ remains almost unchanged up to 900°C. The observed small variations indicate that at a temperature higher than 1100°C, $Mo_{0.975}Ti_{0.025}O_2$ should undergo a phase transition where the double bonds would become either single or be broken completely, in which case the tetragonal rutile structure would be obtained.

Introduction

At room temperature MoO_2, a metallic conductor ($\rho_{298\,K} \simeq 10^{-4}\ \Omega$ cm) and a weak paramagnet, is isostructural with the insulating phase of VO_2, which is monoclinic ($P2_1/c$ space group) and has a rutile-like arrangement. The distortion from the tetragonal symmetry of rutile arises from the M–M pairs which are formed along the c pseudorutile axis. The insulating properties of monoclinic VO_2 are interpreted in terms of these homopolar metal bonds. At the 70°C metal–insulator transition the structure transforms to that of tetragonal rutile with evenly spaced V cation chains and consequently the V–V pairs are broken.

With one more d electron per cation site than VO_2, MoO_2 has one electron available for M–M σ bonding as VO_2, and an additional one to partially fill the M–O π^* band (the conduction band) (*1*). This model which has been confirmed by UV photoelectron spectrum studies (*2*), explains the metallic conductivity of MoO_2 and the Mo–Mo pairs, but it does not shed any light as to

* Permanent address Faculté des Sciences et Techniques de Monastir, Monastir, Tunisia.

† Permanent address: Département de Physique, Université d'Alger, Algeria.

0022-4596/85 $3.00

why the Mo–Mo separation within the pairs is much shorter than expected. As pointed out by Marinder and Magneli (*3*) the Mo–Mo distances across the shared edges correspond to the formation of higher-order bonds. By applying Cotton's empirical correlation of metal–metal distances vs bond order (*4*), Rogers *et al.* (*5*) concluded that the Mo–Mo distance (2.510 Å) observed for MoO_2 is considerably closer to that expected for a bond order of 2. The same result is obtained by applying the empirical relationship suggested by Pauling: $d_2 - d_1 = 0.33 \ln(n_1/n_2)$, where d is the bond distance and n the bond order (*6*). The difference between the ionic radii of Mo^{4+} and V^{4+} can be estimated at about 0.07 Å. The Mo–Mo separation corresponding to a bond order of 1, can be calculated from the V–V distance found in VO_2 (2.619 Å), at 2.76 Å. The difference (2.76 − 2.51 = 0.25 Å) yields $n_1 = 2.1\ n_2$, which indicates that the order of the M–M bonds doubles on going from VO_2 to MoO_2. To explain the electrical conductivity and the double Mo–Mo bonds, Rogers *et al.* (*5*) suggested that for MoO_2 both σ and π metal–metal bonding levels are occupied and that the M–M π interactions have considerable ligand character. As in the Goodenough's model the partial filling of the (M–O)π band is responsible for the electric conductivity.

In order to clarify the unusual behavior of MoO_2 with respect to the other dioxides having the rutile arrangement, we undertook precise structural refinements as a function of temperature. Single-crystal X-ray diffraction intensity data have been collected at 24, 300, 700, and 900°C. The lattice parameters have been measured every 20°C from room temperature to 1100°C. Since all single crystals of pure MoO_2 where found to be twinned, these studies have been carried out on Ti-doped MoO_2. Twinning was not investigated in detail, however, it can be stated qualitatively that the impurity had the effect to change the twinning obliquity and some untwinned crystals were found in each preparation. The incorporation of the Ti^{4+} cations, having the $3d^0$ configuration reduced the electric conductivity, for example, a decrease of about 10% was obtained for a sample containing 2.5% of titanium.

Experimental

The crystal growth technique has been described elsewhere (*7*). A fractured single crystal of $Mo_{0.925}Ti_{0.025}O_2$, shown to be untwinned by precession photographs taken with filtered Mo$K\alpha$ radiation, was ground into a sphere of 0.18 mm in diameter. The $P2_1/c$ space group was confirmed as the precession photographs showed the systematic absences: $h0l$ with $l \neq 2n$ and $0k0$ with $k \neq 2n$. The sphere was then mounted on a Philips four-circle diffractometer. A hot gas (N_2) blower was used to obtain the high temperatures. This attachment is described in detail in Ref. (*8*). The experimental procedure for the intensity data collection is given in Table I. The Lorentz, polarization, and absorption ($\mu R = 0.82$) corrections were applied in order to obtain the structure factors.

The lattice parameters were determined by the use of the same sphere used for the intensity data collections. The θ angles of 25 independent reflections taken in the θ region where the α_1/α_2 doublets are fully separated, were measured every 25 degrees from room temperature up to 1100°C. At room temperature the least-squares refinement yielded the following values: a = 5.609(1), b = 4.860(1), c = 5.628(1) Å, and β = 120.94(1)°. They are to be compared with those published for pure MoO_2 by Brandt and Skapski (*9*): a = 5.6109(8), b = 4.8562(6), c = 5.6285(7) Å, and β = 120.95(1). These values were determined by the use of a Guinier camera, Cu$K\alpha$ radiation, and an internal standard (KCl). The agreement is good for a, c, and β, however,

TABLE I

EXPERIMENTAL PROCEDURE

	Wavelength Scan mode Scan width Scan speed		Graphite monochromated Mo$K\alpha$ ω scan; SM0 2[a] and BM0 2[a] (1.60 + 0.15 tn θ)° 0.1°/sec			
		R.T.	300°C	500°C	700°C	900°C
Number of scans		2	1	1	1	1
All reflections in the θ range (°) were measured		3–48	3–38	3–38	3–38	3–38
Number of reflections measured		4403	2577	2453	2438	2425
Number of reflections used in the refinement		685	354	362	395	362
R		0.020	0.021	0.021	0.021	0.024
wR		0.024	0.024	0.023	0.025	0.028

[a] Code used in the user's manual for the Philips diffractometer.

the b parameters differ by 1/1200. The values of the lattice parameters and of the unit cell volume as a function of temperature are reported in Fig. 1.

The structural refinement were carried out with the Enraf-Nonius SDP system. The f-curves for neutral atoms (the 2.5% Ti was not taken into account) and the coefficients of the anomalous dispersion correction for Mo, were taken from the International Tables for X-Ray Crystallography. The weighting scheme ($w = 1/\sigma(F^2)$) was

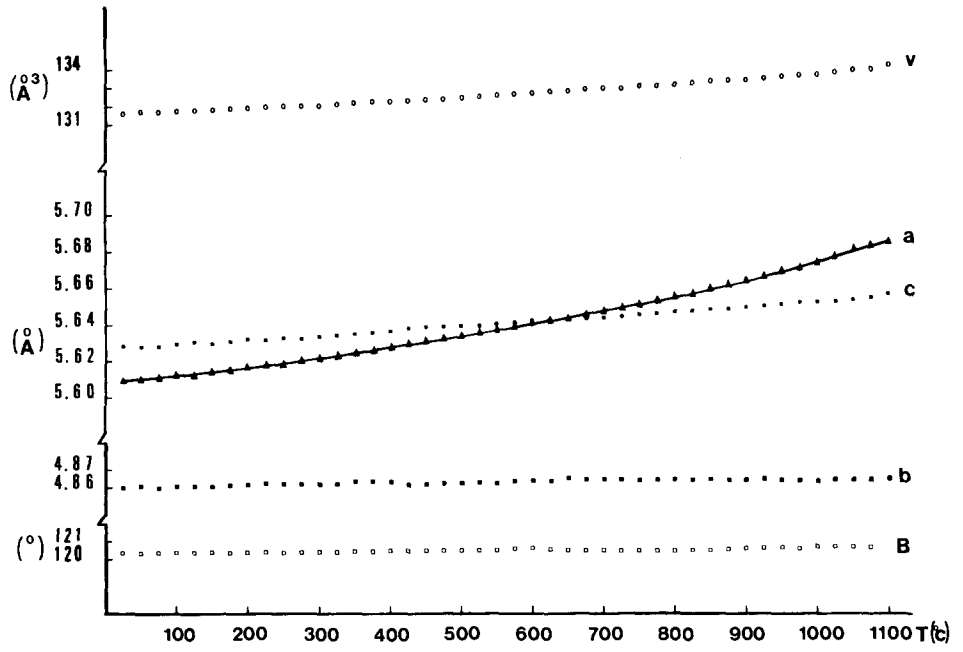

FIG. 1. Lattice parameters and unit cell volume as a function of temperature.

TABLE II

POSITIONAL AND THERMAL PARAMETERS

		x	y	z	U_{11}[a]	U_{22}[a]	U_{33}[a]	U_{12}[a]	U_{13}[a]	U_{23}[a]
R.T.	Mo	.23167(2)	−.00802(2)	.01646(2)	25.2(3)	26.8(3)	23.8(3)	−1.3(2)	13.8(2)	−1.8(2)
	O(1)	.1109(2)	.2165(2)	.2236(2)	44(2)	52(2)	46(2)	−11(2)	26(1)	−22(2)
	O(2)	.3911(2)	.6970(2)	2993(2)	39(2)	53(2)	47(2)	10(2)	24(1)	20(2)
300°C	Mo	.23190(3)	−.00806(2)	.01623(3)	49.1(7)	48.5(6)	45.0(7)	−1.6(3)	3.7(3)	−3.7(3)
	O(1)	.1109(3)	.2167(3)	.2329(3)	73(4)	85(4)	87(4)	25(3)	42(3)	41(3)
	O(2)	.3915(3)	.6973(3)	.2997(3)	71(4)	87(4)	84(4)	20(3)	42(3)	32(3)
500°C	Mo	.23212(3)	−.00815(3)	.01616(3)	63.0(7)	61.4(6)	60.4(7)	−2.6(4)	30.9(6)	−4.2(4)
	O(1)	.1110(3)	.2171(3)	.2329(3)	89(4)	104(5)	104(4)	−23(4)	47(3)	−49(4)
	O(2)	.3918(3)	.6973(3)	.2994(3)	92(4)	114(5)	101(4)	21(4)	53(3)	37(4)
700°C	Mo	.23231(3)	−.00827(3)	.01601(3)	77.7(6)	76.1(6)	76.7(6)	−2.6(4)	39.2(5)	−4.9(4)
	O(1)	.1104(3)	.2181(3)	.2316(3)	118(5)	128(5)	126(5)	−26(4)	66(4)	−55(4)
	O(2)	.3927(3)	.6984(3)	.3003(3)	103(5)	135(5)	127(5)	25(4)	60(4)	43(4)
900°C	Mo	.23278(4)	−.00826(3)	.01602(4)	104(1)	96(1)	72(1)	−4.1(3)	31.3(9)	−6.3(3)
	O(1)	.1102(3)	.2171(4)	.2308(3)	150(5)	162(6)	130(4)	−37(4)	66(4)	−77(4)
	O(2)	.3923(3)	.6989(4)	.3007(3)	145(5)	171(6)	141(4)	28(4)	77(3)	65(4)

[a] Multiplied by 10^4.

that of the SDP system. The starting values for the positional and isotropic parameters at room temperature were those of Brandt and Skapski (*9*). At the higher temperatures, the starting values were the final ones of the previous temperature. There are four formulae per unit cell and all atoms, Mo, O(1), and O(2), are in the general positions. During the last stages of the refinement the anisotropic temperature factors were introduced. The final R and wR values are given in Table I. The positional and thermal parameters are reported in Table II while the interatomic distances and angles are shown in Table III (see Fig. 2). The room-temperature data are in good agreement with those of Brandt and Skapski (*9*). The only significant improvement is in the standard deviations.

Discussion

As stated above, the departure from the rutile structure of MoO_2 and VO_2 is due to the formation of the metal–metal bonds across the shared octahedral edges. The infinite cation chains along the pseudorutile axis are comprised of alternate short and long M–M distances. Although VO_2 and MoO_2 have the same space group symmetry and are thus considered to be isostructural, the different electronic configuration of V^{4+} and Mo^{4+} brings about different structural distortions. In forming the V–V bonds the V^{4+} cations move toward each other along the pseudorutile c axis and twist at the same time in the basal pseudorutile plane. In the case of MoO_2, the paired Mo^{4+} cations are displaced toward each other, but their twisting is not as large as that of the V^{4+} cations. At room temperature, a V^{4+} cation is displaced from the pseudorutile position of 0.137 Å along the c axis and of 0.153 Å in the xy pseudorutile plane. The corresponding displacements of the Mo^{4+} cations are 0.149 and 0.088 Å, respectively.

The octahedral distortion can be defined by the standard deviation calculated for the six M–O distances and/or by that calcu-

TABLE III

INTERATOMIC DISTANCES (Å) AND ANGLES (°)

	R.T.		300°C		500°C		700°C		900°C		R.T.
Mo-Octahedron											VO_2[a]
Mo_3–$O(1)_2$[b]	1.973(1)		1.975(1)		1.975(2)		1.977(2)		1.983(2)		2.017
–$O(1)_3$	1.999(1)		2.000(1)		2.004(2)		2.007(2)		2.006(2)		1.865
–$O(1)_4$	1.980(2)		1.982(1)		1.987(1)		1.990(1)		1.991(1)		1.894
–$O(2)_1$	2.071(1)		2.073(1)		2.076(2)		2.077(2)		2.082(2)		2.025
–$O(2)_2$	2.064(1)		2.065(1)		2.071(2)		2.072(2)		2.071(2)		2.065
–$O(2)_3$	1.981(1)		1.984(1)		1.980(1)		1.984(2)		1.984(2)		1.765
Average	2.011		2.013		2.015_5		2.018		2.019_5		1.939
Distortion coefficient	0.045		0.044		0.046		0.045		0.045		0.116
	Distance	Angle	Distance	Angle	Distance	Angle	Distance	Angle	Distance	Angle	Distance
$O(1)_3$–$O(1)_2$	2.833	91.01(4)	2.836(3)	90.99(6)	2.838(4)	90.99(7)	2.839(4)	90.89(7)	2.843(4)	90.91(7)	2.713
$O(1)_3$–$O(1)_4$	3.087	101.77(4)	3.085(3)	101.54(6)	3.089(4)	101.41(7)	3.088(4)	101.20(7)	3.077(4)	100.71(7)	2.697
$O(1)_3$–$O(2)_3$	2.896	93.38(4)	2.898(2)	93.35(6)	2.898(3)	93.33(7)	2.907(4)	93.48(7)	2.901(4)	93.27(7)	2.749
$O(1)_3$–$O(2)_1$	2.894	90.65(4)	2.897(2)	90.67(6)	2.901(4)	90.59(7)	2.905(4)	90.66(7)	2.915(4)	90.95(7)	2.860
$O(1)_4$–$O(1)_2$	2.779	89.36(4)	2.784(3)	89.40(6)	2.786(4)	89.36(7)	2.790(4)	89.39(7)	2.793(4)	89.30(7)	2.725
$O(1)_4$–$O(2)_3$	2.901	94.18(4)	2.905(2)	94.17(6)	2.908(3)	94.28(7)	2.911(4)	94.22(7)	2.914(4)	94.28(7)	2.741
$O(2)_1$–$O(2)_3$	2.899	91.31(4)	2.901(2)	91.29(6)	2.899(3)	91.21(7)	2.901(4)	91.17(7)	2.907(4)	91.25(7)	2.717
$O(2)_1$–$O(1)_2$	2.709	84.10(4)	2.713(2)	84.11(6)	2.716(3)	84.15(7)	2.719(4)	84.23(7)	2.728(4)	84.24(7)	2.667
$O(2)_2$–$O(1)_4$	2.727	94.78(4)	2.735(2)	85.01(6)	2.745(3)	85.11(7)	2.755(4)	85.39(7)	2.761(4)	85.62(7)	2.893
$O(2)_2$–$O(2)_3$	2.861	89.99(4)	2.863(3)	89.98(6)	2.864(4)	89.96(7)	2.866(4)	89.91(7)	2.868(4)	90.02(7)	2.725
$O(2)_2$–$O(1)_2$	2.732	85.13(4)	2.735(2)	85.18(6)	2.740(4)	85.21(7)	2.742(4)	85.22(7)	2.748(4)	85.23(7)	2.772
$O(2)_2$–$O(2)_1$	2.725	82.44(4)	2.727(2)	82.43(6)	2.736(4)	82.54(7)	2.732(4)	82.40(7)	2.735(4)	82.37(7)	2.590
Standard deviation	0.002	0.004	0.002	0.006	0.004	0.007	0.004	0.007	0.004	0.007	
Average	2.837	89.84	2.840	89.82	2.843	89.85	2.846	89.85	2.849	89.85	2.737
Distortion coefficient	0.110	5.34	0.108	5.26	0.107	5.22	0.106	5.16	0.103	5.05	0.080

[a] Ref. (*10*).

[b] The subscripts refer to Fig. 2.

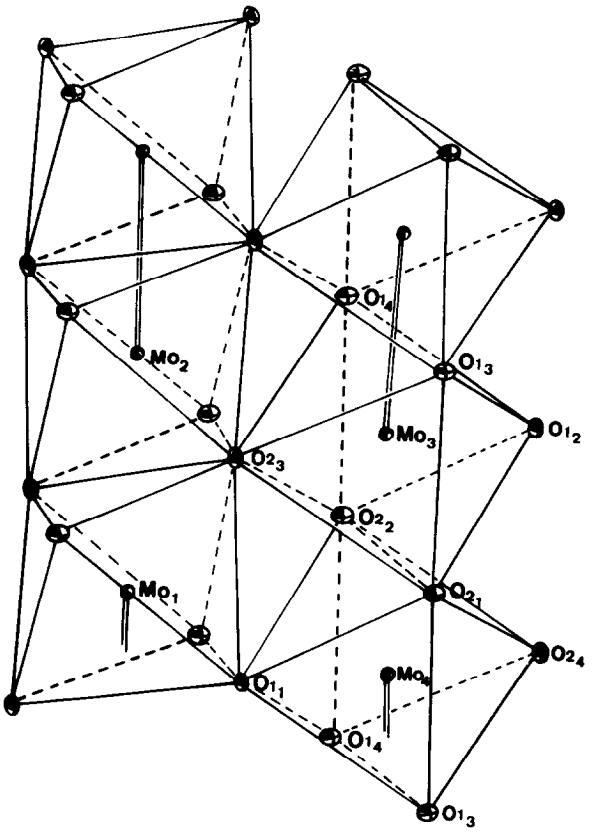

FIG. 2. The structural arrangement of monoclinic rutile-like MoO_2. The atoms are represented by their thermal ellipsoids. The oxygen octahedra around the Mo atoms and the Mo–Mo pairs are outlined. The subscripts 1, 2, 3, and 4 correspond to the positions: xyz; $\bar{x}\bar{y}\bar{z}$; $\bar{x}$, $\frac{1}{2}+y$, $\frac{1}{2}-z$; and x, $\frac{1}{2}-y$, $\frac{1}{2}+z$.

lated for the 12 O–O distances. The former gives information about the distortion due to the cation displacement while the latter gives information about the octahedral shape. The values for $Mo_{0.975}Ti_{0.025}O_2$ and VO_2 are given in Table III. The distortion coefficients calculated from the M–O distances are 0.045 and 0.116 Å for $Mo_{0.975}Ti_{0.025}O_2$ and VO_2, respectively. These values confirm that the Mo^{4+} cations are not displaced from the octahedral centers in contrast to the V^{4+} cations. The distortion coefficients calculated from the O–O distances are 0.110 Å for $Mo_{0.975}Ti_{0.025}O_2$ and 0.080 Å for VO_2. The oxygen octahedra around the Mo^{4+} cations are more distorted than those around the V^{4+} cations due to the rigid Mo–Mo double bonds. It is worth mentioning that the two types of distortion coefficient are not independent; in fact, a displaced cation causes an imbalance in the electrostatic charge and consequently the anions move from their positions in order to reestablish the balance.

The individual bond strengths and the cation and anion valences are reported in Table IV. They have been calculated by the use of the Zachariasen formula $D(s) = D(1)\ (1 - A \ln s)$ where $D(S)$ is the interatomic distance, s the bond strength, $D(1)$ the interatomic distance for unit strength, and A a constant (*11*). The cation (anion)

TABLE IV

BOND STRENGTH AND VALENCES

					MoO_2				
	T (°C)	$O(1)_3$	$O(1)_2$	$O(1)_4$	$O(2)_2$	$O(2)_1$	$O(2)_3$	Σs_C	$D(1)$
Mo	R.T.	.689	.748	.732	.558	.546	.728	4.001	1.882
Σs_A			2.169			1.832			
	300	.689	.746	.730	.560	.547	.727	3.999	1.884
Σs_A			2.165			1.834			
	500	.685	.753	.724	.554	.545	.740	4.001	1.886
Σs_A			2.162			1.839			
	700	.684	.753	.723	.736	.556	.548	4.000	1.888
Σs_A			2.160			1.840			
	900	.690	.742	.725	.740	.561	.542	4.000	1.890
Σs_A			2.157			1.843			
					VO_2[a]				
V	R.T.	0.794	0.723	0.494	1.089	0.480	0.424	4.004	1.790
Σs_A			2.011			1.993			

[a] Calculated by using the data of Ref. (*10*).

charges have been calculated by summing the bond strengths over the anions (cations) surrounding each cation (anion). A striking feature is that this calculation gives 4.00 for the Mo cations whereas it gives 2.17 and 1.83 for the O(1) and O(2), respectively. This imbalance indicates that the O(1) are strongly overbonded while the O(2) are strongly underbonded. The octahedral shared edges, across which the Mo–Mo pairs are formed, are comprised of two O(1), which may cause the O(1) to be overbonded. The same type of calculation applied to VO_2 gives 4.00, 2.01, and 1.99 for the charges of the V, O(1), and O(2) atoms, respectively. This implies that in this case the distortion of the oxygen octahedra fully compensates the V–V pair formation. As stated above, the oxygen octahedra of $Mo_{0.975}Ti_{0.025}O_2$ are more distorted than those of VO_2. However, the distortion is not large enough to counterbalance the double Mo–Mo bonds and unrealistic charges for the two oxygen anions are obtained. The bond length–bond strength method takes into account only cation–anion interactions. The fact that it fails to generate the proper anion charges for $Mo_{0.975}Ti_{0.025}O_2$, can be taken as an indication that the Mo–Mo interactions are of the same order of magnitude as the M–O interactions and therefore they should be taken into consideration. These results strongly corroborate the assumption that the cation–cation bonds in VO_2 and MoO_2 do not have the same bond order and consequently the two compounds should be considered as isostructural only from the topological point of view.

The structural refinements at 300, 500, 700, and 900°C, show that the structure of $Mo_{0.975}Ti_{0.025}O_2$ remains almost unchanged up to 900°C. However, some small, but significant variations are observed. While the (M–O) distortion coefficient remains constant, that of the (O–O) distances decreases slightly from 0.110 Å at room temperature to 0.103 Å at 900°C. Although the (O–O) distortion coefficient decreases, the oxygen charge imbalance also decreases with increasing temperature. The charge of O(1) decreases from 2.168 to 2.159 on going from

room temperature to 900°C, while that of O(2) increases from 1.832 to 1.846 between the same temperatures. These variations indicate that at a temperature well above 900°C, $Mo_{0.975}Ti_{0.025}O_2$ should undergo an electronic transition where the double bonds should become single or be broken completely and the imbalance of the oxygen charge would disappear. The octahedral distortion and the oxygen charge imbalance decrease simultaneously because the increase of the short Mo–Mo distances with increasing temperature is larger than the increase calculated by a modified Debye function such as $D_t = D_{297}\sqrt[3]{V_t/V_{297}}$. Figure 3 illustrates the comparison between the experimental (curve a) and the calculated values (curve b). The value of 2.550 Å for the short Mo–Mo distance at 900°C shows that the double bond still exists at this temperature.

The variation of the lattice parameters as a function of temperature is shown in Fig. 1. The linear thermal expansion coefficient is quite anisotropic as the a_M parameter increases 1.4% between room temperature and 1100°C while the b_M parameter is practically constant between the same temperatures. The a_M axis corresponds to the pseudorutile c_R axis, that is the axis of the Mo–Mo pairs. The increase of the short Mo–Mo distances is greater than that of the a_M parameter. For example, between room temperature and 900°C the a_M parameter increases 1% while the short Mo–Mo distance increases 1.6%.

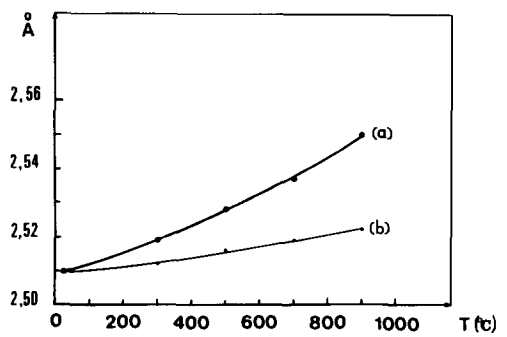

FIG. 3. The experimental variation of the short Mo–Mo distance as a function of temperature (°C) (curve a) and the calculated one according to the function $D_t = D_{297}\sqrt[3]{V_t/V_{297}}$ (curve b).

The thermal parameters reported in Table II show that the thermal vibrations of the Mo atoms are isotropic up to 700°C. The difference between the major and the minor axes of the thermal ellipsoid is 0.006 Å at room temperature and remains constant up to 700°C. At 900°C, this difference increases to 0.021 Å which still corresponds to a somewhat weak anisotropy. The thermal vibrations of the two oxygen atoms O(1) and O(2) are already anisotropic at room temperature where the differences between the major and the minor axes of the thermal ellipsoids are 0.033 and 0.030 Å, respectively. These differences increase linearly with increasing temperature up to 700°C, where the values are 0.050 Å for O(1) and 0.040 Å for O(2). At 900°C they become 0.068 and 0.055 Å, respectively, which are somewhat larger than the values calculated by a linear extrapolation.

It is worthwhile to look at the pseudosymmetry relationship which exists between the thermal ellipsoids of O(1) and O(2). These two atoms are crystallographically independent in the monoclinic structure while they are equivalent in the tetragonal structure. The ellipsoidal axis lengths (rms) in Ångstroms and the angles between these axes and the monoclinic axes, for Mo, O(1), and O(2) at room temperature are given in Table V. It can be seen that the orientation of the O(1) and O(2) ellipsoids is the same within less than 10° if one applies the transformation O(1): $xyz \rightarrow$ O(2): $\frac{1}{2} - x$, $\frac{1}{2} + y$, $\frac{1}{2} - z$. Although the corresponding data at higher temperatures are not reported here, it can be calculated from the data of Table II that the pseudosymmetry relationship between the thermal ellipsoids of O(1) and O(2) remains unchanged up to 900°C.

TABLE V

THERMAL DATA AT ROOM TEMPERATURE

	rms (Å)	Angle with a_M	Angle with b_M	Angle with c_M
Mo	0.053	106.4	33.6	105.3
	0.050	45.4	58.9	86.6
	0.047	130.9	78.7	15.7
O(1)	0.085	92.5	41.5	123.0
	0.063	11.1	81.0	114.1
	0.052	100.8	50.0	42.8
O(2)	0.084	90.8	40.4	55.8
	0.060	3.0	91.2	118.2
	0.054	92.9	130.3	47.3

Conclusions

We have confirmed that in the monoclinic rutile-like $Mo_{0.975}Ti_{0.025}O_2$ structure the Mo–Mo pairs across the shared octahedral edges, correspond to bond order 2. Because of these strong bonds, the bond strength–bond length method fails to yield the correct anion valences. Since the cation–cation pairs have different bond orders in VO_2 and MoO_2, they cause different structural distortions. Therefore, the two dioxides are to be considered as isostructural only from the topological point of view.

The high-temperature structural refinements show that the structure of $Mo_{0.975}Ti_{0.025}O_2$ remains practically unchanged up to 900°C. However, small but significant variations indicate that at a temperature greater than 1100°C, it should undergo either an electronic phase transition, where the pairs would decrease their bond order, or to a crystallographic phase transition, where the symmetry would become tetragonal and the pairs would be broken completely.

References

1. J. B. GOODENOUGH, *Prog. Solid State Chem.* **5,** 145 (1971); *J. Solid State Chem.* **3,** 490 (1971).
2. N. BEETHAM AND A. F. ORCHARD, *J. Electron Spectrosc. Relat. Phenom.* **16,** 77 (1976).
3. B. O. MARINDER AND A. MAGNELI, *Acta Chem. Scand.* **11,** 1635, 1957; **12,** 1345 (1958).
4. F. A. COTTON, *Quant. Rev. (London)* **20,** 389 (1966).
5. D. B. ROGERS, R. D. SHANNON, A. W. SLEIGHT, AND J. L. GILLSON, *Inorg. Chem.* **8,** 841 (1969).
6. L. PAULING, "The Nature of the Chemical Bond," Cornell Univ. Press Ithaca (1960).
7. J. MERCIER, G. FOURCAUDOT, Y. MONTEIL, C. BEC, AND R. HILLEL, *J. Cryst. Growth* **59,** 599 (1982).
8. R. ARGOUD AND J. J. CAPPONI, *J. Appl. Crystallogr.* **17,** 420 (1984).
9. B. G. BRANDT AND A. C. SKAPSKI, *Acta Chem. Scand.* **21,** 661 (1967).
10. J. M. LONGO AND P. KIERKEGAARD, *Acta Chem. Scand.* **24,** 420 (1970).
11. W. H. ZACHARIASEN, *J. Less-Common Met.* **62,** 1 (1978).